

Structure of Immature West Nile Virus[∇]

Ying Zhang, Bärbel Kaufmann, Paul R. Chipman, Richard J. Kuhn, and Michael G. Rossmann*

Department of Biological Sciences, Purdue University, 915 W. State Street, West Lafayette, Indiana 47907-2054

Received 5 January 2007/Accepted 8 March 2007

The structure of immature West Nile virus particles, propagated in the presence of ammonium chloride to block virus maturation in the low-pH environment of the *trans*-Golgi network, was determined by cryo-electron microscopy (cryo-EM). The structure of these particles was similar to that of immature West Nile virus particles found as a minor component of mature virus samples (naturally occurring immature particles [NOIPs]). The structures of mature infectious flaviviruses are radically different from those of the immature particles. The similarity of the ammonium chloride-treated particles and NOIPs suggests either that the NOIPs have not undergone any conformational change during maturation or that the conformational change is reversible. Comparison with the cryo-EM reconstruction of immature dengue virus established the locations of the N-linked glycosylation sites of these viruses, verifying the interpretation of the reconstructions of the immature flaviviruses.

West Nile virus, dengue virus, yellow fever virus, and tick-borne encephalitis virus, members of the *Flaviviridae* family (10), are enveloped viruses with single-stranded RNA genomes. West Nile virus infections in the United States (9) resulted in more than 140 deaths in 2006 (<http://www.cdc.gov/ncidod/dvbid/westnile>).

Genomic RNA replicated in the cytoplasm associates with the capsid (C) protein during the viral life cycle. Immature flavivirus particles are formed when these nucleocapsid cores acquire their lipid envelope together with these membrane-anchored envelope (E) protein and the precursor membrane (prM) protein during the process of budding into the lumen of the endoplasmic reticulum (ER). The prM and E proteins exist as trimers of heterodimers on the surface of the immature particles (19), which then pass through the *trans*-Golgi network (TGN). The E and prM proteins become glycosylated in the ER, albeit at different residues for West Nile and dengue viruses. The fusion peptide on the E protein is protected from premature fusion with membranes in the cell by being covered with the amino-terminal precursor peptide pr (19), rendering the immature particles noninfectious. The maturation process is activated by furin cleavage of the prM protein after exposure to acidic pH, which results in the release of the precursor peptide (16).

The maturation of flaviviruses can be inhibited by growing the viruses in a medium containing the acidotropic agent NH₄Cl, allowing the accumulation of immature virus particles for structural studies (14). The immature dengue virus and yellow fever virus particles, produced by adding NH₄Cl to the medium (ammonium chloride-treated immature particles [ACIPs]), have diameters of about 600 Å, with trimers of prM-E heterodimers arranged icosahedrally, forming 60 protruding spikes on the surface of each particle (19). In contrast, mature infectious virus particles contain 90 E-E homodimers that form a much

smoother surface and these particles have diameters of only about 500 Å (12, 17). Without visualizing any intermediate states in virus maturation, the large conformational changes that must occur are difficult to comprehend (Fig. 1). It is, therefore, essential to determine that the immature structure, as described by Zhang et al. (19), is, indeed, a true structural intermediate in the life cycle of the virus.

Organization of immature West Nile virus. A three-dimensional, 24-Å-resolution, cryo-electron microscopy (cryo-EM) reconstruction of the West Nile virus ACIPs (Table 1; Fig. 2A) showed surface features similar to those of dengue virus ACIPs (19). The surface of the virus is dominated by 60 icosahedrally arranged trimeric glycoprotein spikes, as is the surface of naturally occurring immature particles (NOIPs) (Fig. 2C). Cross-sectional views of the reconstruction show a multilayered structure composed of the prM and E glycoproteins (between 199 and 287 Å radius), a lipid bilayer (167 to 199 Å radius), and the nucleocapsid core (within a radius of 167 Å), as also seen in NOIPs (Fig. 2D). Similar to that of dengue virus, the nucleocapsid core does not show well-ordered structural features on the icosahedrally averaged cryo-EM map.

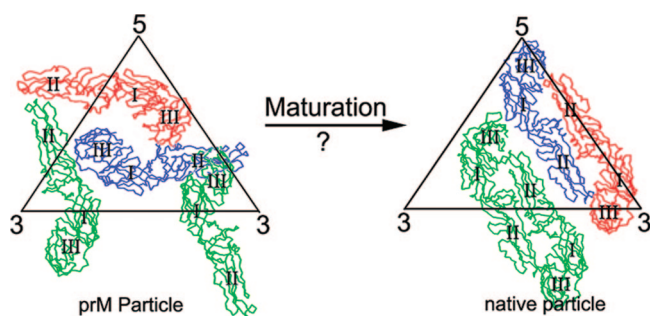


FIG. 1. Diagram showing the structural rearrangement required for immature particles to become mature particles. The C α backbones of the three independent E molecules per icosahedral asymmetric unit are colored green, red, and blue. The three domains in each E molecule are labeled I, II, and III. (Reprinted from the *EMBO Journal* [19] with permission of the publisher.)

* Corresponding author. Mailing address: Department of Biological Sciences, Purdue University, 915 W. State St., West Lafayette, IN 47907-2054. Phone: (765) 494-4911. Fax: (765) 496-1189. E-mail: mr@purdue.edu.

[∇] Published ahead of print on 21 March 2007.

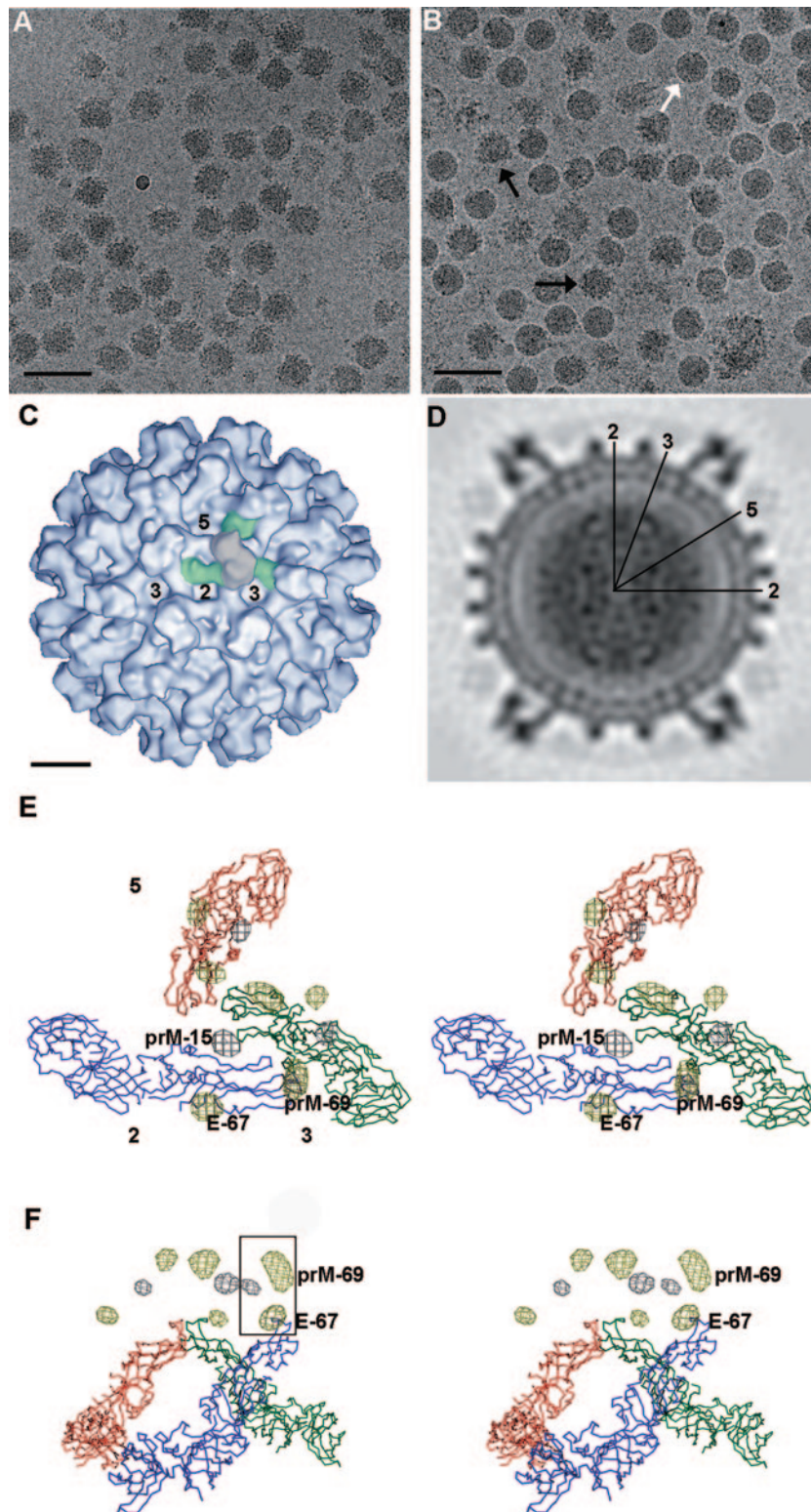


FIG. 2. Cryo-EM micrographs, density maps, and difference density maps showing the positions of carbohydrate sites. (A) Cryo-EM micrograph of West Nile virus ACIPs. Immature particles were produced from cells treated with ammonium chloride. Confluent Vero cells were infected with West Nile virus at a multiplicity of infection of 1.0 in the presence of 2% fetal calf serum. At 22 h after infection, the cell culture medium was exchanged with medium containing 20 mM NH_4Cl . This first overlay was discarded at 23 h after infection and replaced with fresh NH_4Cl -containing medium. The cell culture supernatant was harvested 48 h after infection, and immature virus was purified as described previously for mature particles (8). Cryo-EM micrographs showed that the ammonium chloride-treated preparation consisted almost exclusively of immature particles (ACIPs). Sodium dodecyl sulfate-polyacrylamide gel electrophoresis (SDS-PAGE) of these ACIPs showed that the majority of the prM protein was uncleaved. (B) Cryo-EM micrograph of West Nile virus particles produced without NH_4Cl . Black arrows point to NOIPs, whereas the

TABLE 1. Cryo-EM image reconstruction data^a

Type of virus particle	No. of micrographs	Defocus (μm)	No. of particles	PFT CC ^b	Resolution (Å)
NOIPs ^c	45	1.3–3.1	341	0.288	24
ACIPs ^d	39	1.2–3.3	720	0.261	24

^a Images were recorded with an FEI Philips CM300 transmission electron microscope at a calibrated magnification of $\times 47,400$. Micrographs were digitized with a Zeiss-PHODIS scanner to yield a sampling corresponding to 2.95 Å between pixels on the specimen.

^b PFT CC is the correlation coefficient (CC) between the model projection and the corresponding raw image after polar Fourier transformation (PFT) (1).

^c West Nile virus NOIPs were centered and classified as described by Furst et al. (6) but using the program SPIDER (5). The self-common line method (2) was then applied to the class averages to generate an initial model for the subsequent reconstruction of the NOIP data as for the reconstruction of the West Nile virus ACIP data.

^d The reconstruction of West Nile virus ACIPs was performed with the cryo-EM image reconstruction of dengue virus ACIPs as a starting model by using the PFT procedure (1).

Since the hinge angle between domains I and II of the E protein is a little different in mature and immature dengue virus particles (20), the fitting of each domain into the cryo-EM map should be performed independently. However, this approach was not reasonable because of the relatively low resolution of the current West Nile virus reconstruction. Hence, the atomic structure of the West Nile virus E protein (7, 13) was fitted, as a single rigid body, into the cryo-EM density map of immature West Nile virus by using the program EMfit (15) (Table 2). Three E monomers could be positioned into each icosahedral asymmetric unit. Like that of the E proteins in immature dengue virus particles, the organization of the E proteins in West Nile virus does not conform to classical T=3 quasiasymmetry (3). The three E molecules within each spike of the immature particles are tilted with respect to the viral surface, with their fusion peptides pointing toward the tip of the spike. The fusion peptides are covered by extra density, attributed to the prM protein.

Glycosylation sites in immature particles. The West Nile and dengue virus glycoproteins have 46% sequence identity. West Nile virus has two potential glycosylation sites (at E protein residue 154 [E-154] and prM protein residue 15 [prM-15]) on each prM-E heterodimer that differ from the glycosylation sites of immature dengue virus (at E-67, E-153, and prM-69). A 24-Å-resolution difference map, computed as the immature West Nile virus density minus the immature dengue virus density, showed three strong positive and six strong negative well-defined density peaks per icosahedral asymmetric unit, with magnitudes roughly 1.5 times as large as any other

TABLE 2. Fitting of the E glycoprotein X-ray structure into the cryo-EM map^a

Molecule ^b	sumf1 ^c (%)	sumf2 ^c (%)	sumf3 ^c (%)	-den ^d (%)	clash ^e (%)	centx ^f (Å)	centy ^f (Å)	centz ^f (Å)
Green	50.6	59.0	51.2	0.0	0.2	33.1	-84.5	201.5
Red	48.5	56.4	49.3	0.0	0.0	92.2	-46.6	196.5
Blue	54.3	57.6	50.6	0.2	0.0	33.2	-4.4	220.5

^a The C α backbone of the West Nile virus E molecule (Protein Data Bank accession number, 2HG0) was used to fit into the NOIP and ACIP electron density maps with a procedure described by Zhang et al. (19) and Rossmann et al. (15). The pixel size of the ACIP and NOIP West Nile virus maps was adjusted with respect to the cryo-EM map of immature dengue virus by minimizing the root mean square difference in density within the external protein layer (between 190 and 290 Å radius). The cryo-EM densities on the two magnification-adjusted maps were then put onto the same relative scale by minimizing the function $\sum(\rho_{den} - a\rho_{WN} - b)^2$ by using density values within the external protein region, where a and b are scale factors and ρ_{den} and ρ_{WN} are the density values for the dengue and West Nile virus immature particles, respectively. After having established both the magnification and density scale factors, the difference map between the dengue and West Nile virus immature particles was computed.

^b Molecule refers to the green, red, and blue color coding in Fig. 1 and 2E and F.

^c sumf1, sumf2, and sumf3 are the average densities at C α atoms for domains I, II, and III, respectively, expressed as percentages of the highest density in the map.

^d -den is the percentage of atoms in negative density.

^e clash is the percentage of atoms that sterically interfere between neighboring molecules.

^f centx, centy, and centz are the coordinates of the center of mass of the E monomer in the map.

positive or negative peaks. The three positive peaks obey the symmetry of the three prM-E heterodimers within each icosahedral asymmetric unit and can be attributed to the carbohydrate moieties associated with the prM protein (at prM-15) in West Nile virus. The six negative peaks within each icosahedral asymmetric unit can be divided into two sets of three peaks. The spatial relationship among the three peaks of each set is consistent with that among the three E monomers (Fig. 2E and F). Thus, there are two negative peaks associated with each prM-E heterodimer, presumably corresponding to the glycosylation sites at E-67 and prM-69 in dengue virus. The centers of one set of negative difference density peaks are about 17 Å from the corresponding C α atoms of the glycosylated asparagines (at E-67) and well outside the density of the fitted E proteins. This distance is comparable to distances found in a study of carbohydrate sites in Sindbis virus (18), confirming the correct handedness of the cryo-EM map of immature West Nile virus and dengue virus particles, as well as the fitting of the E molecules into the cryo-EM map (Table 3). The other negative glycosylation site must correspond to the carbohydrate moiety at prM-69 of dengue virus. The West Nile virus

white arrow points to mature particles. Scale bars in both panels A and B represent 1,000 Å. Mature West Nile virus (NY99) was propagated and purified as described elsewhere (8), except that the virus was harvested 30 h after infection and concentrated by polyethylene glycol precipitation. The analysis of these particles by SDS-PAGE showed the presence of E, C, and prM proteins, as well as M proteins. Cryo-EM showed that up to one in five particles in the resulting preparations was an immature-looking particle. (C) Surface representation of NOIPs. Icosahedral 5-, 3-, and 2-fold axes are labeled. In one spike, prM protein is colored gray and E protein is colored green. The scale bar represents 100 Å. (D) Central cross-section showing the multilayer organization of West Nile virus NOIPs. Icosahedral symmetry operators are indicated with black lines. (E) Stereo view of a spike showing the difference density between West Nile virus and dengue virus ACIPs. The C α backbone of the E molecules is shown in green, red, and blue. Positive and negative peaks are colored gray and yellow, respectively. The icosahedral 5-, 3-, and 2-fold axes are labeled. The N-linked glycosylation sites (Asn-15 in the prM protein of West Nile virus [prM-15], Asn-67 in the E protein of dengue virus [E-67], and Asn-69 in the prM protein of dengue virus [prM-69]) associated with the difference densities are labeled. (F) Stereo view showing the same difference map as panel E but from a side view. The three difference density peaks associated with one prM-E heterodimer are outlined with a black rectangle.

TABLE 3. Positions of the highest difference map density peaks corresponding to carbohydrate moieties

Virus	Glycosylation site	Molecule ^a	x ^b (Å)	y ^b (Å)	z ^b (Å)	Distance ^c (Å)
West Nile	prM-15	Green	47.3	-77.7	260.1	
		Red	86.1	-45.9	258.3	
		Blue	43.7	-39.4	269.7	
Dengue	prM-69	Green	61.3	-54.2	271.6	
		Red	70.1	-32.4	276.3	
		Blue	30.9	-64.0	273.3	
	E-67	Green	61.1	-76.9	244.4	15.5
		Red	94.5	-30.1	247.0	17.3
		Blue	19.9	-32.3	261.5	17.6

^a Molecule refers to the green, red, and blue color coding in Fig. 1 and 2E and F.

^b The x, y, and z coordinates of the centers of difference density peaks between West Nile virus and dengue virus immature particles are shown.

^c The distance between the center of the difference density peak and the corresponding C α atom of the fitted E X-ray structure.

glycosylation site at E-154 (which should give a positive peak in the difference map) is structurally aligned with that at E-153 in dengue virus (which should produce a negative peak). As there is no significant peak in the difference map near these residues, it appears that these two peaks have cancelled each other out.

Naturally occurring immature particles resemble immature particles produced by NH₄Cl. The preparation of West Nile virus in Vero cells is a mixture of both mature (smaller and smoother)- and immature (larger and spikier)-looking particles, as observed in cryo-EM micrographs (Fig. 2B), which could not be separated by additional purification steps. About 20% of the manually selected spiky particles converged into a structure described here. The rejected particles probably have an intermediate conformation between those of mature and immature virus particles. The 24-Å-resolution cryo-EM reconstruction of these NOIPs (Fig. 2C) is similar to that of the ACIPs, with a root mean square deviation of 2.9 Å between equivalent C α atoms of the fitted E molecules. The biggest peaks on the NOIP or ACIP cryo-EM map were three times as large as the biggest peak on the (NOIP-ACIP) difference map. Furthermore, the biggest density peak in the (NOIP-ACIP) difference map was only about three times the root mean square deviation of the density from the mean for the difference map as a whole. Thus, there was no significant difference between these two types of particles at the resolution attained in this study. In addition, the radially averaged correlation

between the densities in the two maps, computed as a function of the distance from the center of the particles, showed that the glycoprotein and lipid layers are essentially identical. Thus, the structure of ACIPs is likely to be the true state of the immature particles and is not the result of an artifact created by the NH₄Cl treatment.

Immature virus particles pass from an environment of neutral pH in the ER to one of acidic pH in the TGN (4, 11) and then, after maturation, back to neutral pH upon exiting the host cell (Table 4, pathways A to D). The large conformational change that occurs during maturation might be caused when entering the low-pH environment of the TGN, when exiting from the TGN (14), or by a combination of both these transitions. The ACIPs are presumably produced because the NH₄Cl blocks the maturation of virus particles by raising the pH of the TGN to inhibit either a putative conformational change (16) upon entrance into the TGN and/or the subsequent cleavage of the prM protein. The inhibition of the pH-induced, putative conformational change might stop the exposure of the cleavage site (Table 4, pathway G), or the inhibition of the prM protein cleavage might alter the subsequent conformational changes that are required for maturation (Table 4, pathway F). Both the ACIPs and NOIPs contain uncleaved prM protein, suggesting that the NOIPs must have bypassed the cleavage process. Furthermore, the structures of the ACIPs and the NOIPs are very similar. The NOIPs might not have undergone any conformational change upon entering the TGN (Table 4, pathway B), might have gone through a reverse conformational change upon leaving the TGN (Table 4, pathway D), or might have been released by cytopathic effects without passing the acidic TGN (Table 4, pathway E). However, a low-pH-induced conformational change has been shown to be irreversible for tick-borne encephalitis virus (16). In contrast, particles that are missing the precursor peptide will continue on the pathway to maturation (Table 4, pathways A and C). A lack of cleavage or a lack of conformational change, whichever might be the reason for the production of NOIPs, might be the result of insufficient time of residence in the acidic-pH environment of the TGN, or local variability of pH in the TGN, to permit the complete maturation process.

Accession numbers. The electron density map of West Nile virus NOIPs was deposited with the Electron Microscopy Data Bank (accession number EMD-1314). The fitted model of E molecules was deposited with the Protein Data Bank (accession number 2OF6).

TABLE 4. Possible maturation pathways of flavivirus particles

Growth condition	Pathway, starting with assembled particles in the ER at neutral pH	Conformational change \Rightarrow	Cleavage event in TGN at acidic pH	Conformational change \Rightarrow	Type of particles released into neutral-pH environment
No NH ₄ Cl	A	No	prM cleavage	Yes	Mature virus
	B	No	No prM cleavage	No	NOIPs
	C	Yes	prM cleavage	Yes	Mature virus
	D	Yes	No prM cleavage	Reverse change	NOIPs
	E	NA ^a	TGN bypassed	NA	NOIPs
NH ₄ Cl added	F	No	Blocked cleavage	No	ACIPs
	G	Blocked	No cleavage	No	ACIPs

^a NA, not applicable.

We thank Jue Chen for many helpful discussions and Cheryl Towell, Sheryl Kelly, and Sharon Wilder for help in preparing the manuscript. Figures were made using the programs DINO: Visualizing Structural Biology (2002; <http://www.dino3d.org>) and RobEM (<http://cryoem.ucsd.edu/programDocs/runRobem.txt>).

The work was supported by a National Institutes of Health Program Project grant (AI 55672) to M.G.R. and R.J.K. and an award from the Keck Foundation for the purchase of the CM300 transmission electron microscope used in this study.

REFERENCES

1. Baker, T. S., and R. H. Cheng. 1996. A model-based approach for determining orientations of biological macromolecules imaged by cryoelectron microscopy. *J. Struct. Biol.* **116**:120–130.
2. Baker, T. S., N. H. Olson, and S. D. Fuller. 1999. Adding the third dimension to virus life cycles: three-dimensional reconstruction of icosahedral viruses from cryo-electron micrographs. *Microbiol. Mol. Biol. Rev.* **63**:862–922.
3. Caspar, D. L. D., and A. Klug. 1962. Physical principles in the construction of regular viruses. *Cold Spring Harbor Symp. Quant. Biol.* **27**:1–24.
4. Demarex, N., W. Furuya, S. D'Souza, J. S. Bonifacio, and S. Grinstein. 1998. Mechanism of acidification of the *trans*-Golgi network (TGN). *J. Biol. Chem.* **273**:2044–2051.
5. Frank, J., M. Radermacher, P. Penczek, J. Zhu, Y. Li, M. Ladjadj, and A. Leith. 1996. SPIDER and WEB: processing and visualization of images in 3D electron microscopy and related fields. *J. Struct. Biol.* **116**:190–199.
6. Furst, J., R. B. Sutton, J. Chen, A. T. Brunger, and N. Grigorieff. 2003. Electron cryomicroscopy structure of *N*-ethyl maleimide sensitive factor at 11 Å resolution. *EMBO J.* **22**:4365–4374.
7. Kanai, R., K. Kar, K. Anthony, L. H. Gould, M. Ledizet, E. Fikrig, W. A. Marasco, R. A. Koski, and Y. Modis. 2006. Crystal structure of West Nile virus envelope glycoprotein reveals viral surface epitopes. *J. Virol.* **80**:11000–11008.
8. Kaufmann, B., G. E. Nybakken, P. R. Chipman, W. Zhang, M. S. Diamond, D. H. Fremont, R. J. Kuhn, and M. G. Rossmann. 2006. West Nile virus in complex with the Fab fragment of a neutralizing monoclonal antibody. *Proc. Natl. Acad. Sci. USA* **103**:12400–12404.
9. Lanciotti, R. S., J. T. Roehrig, V. Deubel, J. Smith, M. Parker, K. Steele, B. Crise, K. E. Volpe, M. B. Crabtree, J. H. Scherret, R. A. Hall, J. S. MacKenzie, C. B. Cropp, B. Panigrahy, E. Ostlund, B. Schmitt, M. Malkinson, C. Banet, J. Weissman, N. Komar, H. M. Savage, W. Stone, T. McNamara, and D. J. Gubler. 1999. Origin of the West Nile virus responsible for an outbreak of encephalitis in the northeastern United States. *Science* **286**:2333–2337.
10. Lindenbach, B. D., and C. M. Rice. 2001. *Flaviviridae*: the viruses and their replication, p. 991–1041. In D. M. Knipe and P. M. Howley (ed.), *Fields virology*, 4th ed. Lippincott Williams & Wilkins, Philadelphia, PA.
11. Llopis, J., J. M. McCaffery, A. Miyawaki, M. G. Farquhar, and R. Y. Tsien. 1998. Measurement of cytosolic, mitochondrial and Golgi pH in single living cells with green fluorescent proteins. *Proc. Natl. Acad. Sci. USA* **95**:6803–6808.
12. Mukhopadhyay, S., B. S. Kim, P. R. Chipman, M. G. Rossmann, and R. J. Kuhn. 2003. Structure of West Nile virus. *Science* **302**:248.
13. Nybakken, G. E., C. A. Nelson, B. R. Chen, M. S. Diamond, and D. H. Fremont. 2006. Crystal structure of the West Nile virus envelope glycoprotein. *J. Virol.* **80**:11467–11474.
14. Randolph, V. B., G. Winkler, and V. Stollar. 1990. Acidotropic amines inhibit proteolytic processing of flavivirus prM protein. *Virology* **174**:450–458.
15. Rossmann, M. G., R. Bernal, and S. V. Pletnev. 2001. Combining electron microscopic with X-ray crystallographic structures. *J. Struct. Biol.* **136**:190–200.
16. Stadler, K., S. L. Allison, J. Schlich, and F. X. Heinz. 1997. Proteolytic activation of tick-borne encephalitis virus by furin. *J. Virol.* **71**:8475–8481.
17. Zhang, W., P. R. Chipman, J. Corver, P. R. Johnson, Y. Zhang, S. Mukhopadhyay, T. S. Baker, J. H. Strauss, M. G. Rossmann, and R. J. Kuhn. 2003. Visualization of membrane protein domains by cryo-electron microscopy of dengue virus. *Nat. Struct. Biol.* **10**:907–912.
18. Zhang, W., S. Mukhopadhyay, S. V. Pletnev, T. S. Baker, R. J. Kuhn, and M. G. Rossmann. 2002. Placement of the structural proteins in Sindbis virus. *J. Virol.* **76**:11645–11658.
19. Zhang, Y., J. Corver, P. R. Chipman, W. Zhang, S. V. Pletnev, D. Sedlak, T. S. Baker, J. H. Strauss, R. J. Kuhn, and M. G. Rossmann. 2003. Structures of immature flavivirus particles. *EMBO J.* **22**:2604–2613.
20. Zhang, Y., W. Zhang, S. Ogata, D. Clements, J. H. Strauss, T. S. Baker, R. J. Kuhn, and M. G. Rossmann. 2004. Conformational changes of the flavivirus E glycoprotein. *Structure* **12**:1607–1618.